International Journal of Thermophysics, Vol. 22, No. 3, 2001

Phase Equilibria of CFC Alternative Refrigerant Mixtures: 1,1,1,2,3,3,3-Heptafluoropropane (HFC-227ea) + Difluoromethane (HFC-32), + 1,1,1,2-Tetrafluoroethane (HFC-134a), and + 1,1-Difluoroethane (HFC-152a)

J.-Y. Park,[1] J. S. Lim,[1,2] B.-G. Lee,[1] and Y.-W. Lee[1]

Received September 6, 2000

Isothermal vapor–liquid equilibria were measured for the binary systems difluoromethane (HFC-32) + 1,1,1,2,3,3,3-heptafluoropropane (HFC-22ea) and 1,1-difluoroethane (HFC-152a) + 1,1,1,2,3,3,3-heptafluoropropane at 283.15 and 303.15 K and 1,1,1,2-tetrafluoroethane (HFC-134a) + 1,1,1,2,3,3,3-heptafluoropropane at 303.15 and 323.15 K in an apparatus in which both phases were recirculated. The experimental data were correlated with the Peng–Robinson equation of state using the Wong–Sandler mixing rules. Azeotropic behavior has not been found in any of the three mixtures.

KEY WORDS: binary mixtures; HFC-227ea; HFC-32; HFC-134a; HFC-152a; Peng–Robinson equation of state; vapor–liquid equilibria; Wong–Sandler mixing rule.

1. INTRODUCTION

Hydrofluorocarbons (HFCs) such as 1,1,1,2,3,3,3-heptafluoropropane (HFC-227ea), difluoromethane (HFC-32), 1,1-difluoroethane (HFC-152a), and 1,1,1,2-tetrafluoroethane (HFC-134a) are promising alternative refrigerants to replace dichlorodifluoromethane (CFC-12; CCl_2F_2) and chlorodifluoromethane (HCFC-22; $CHClF_2$). Their ozone depletion potentials (ODP) are zero since they do not contain chlorine. Their global warming potentials (GWP) are less than those of CFC-12 and HCFC-22 because

---

[1] Division of Environment and Process Technology, Korea Institute of Science and Technology (KIST), P.O. Box 131, Cheongryang, Seoul 130-650, Korea.

[2] To whom correspondence should be addressed. E-mail: limjs@kist.re.kr

0195-928X/01/0500-0901$19.50/0

they contain more hydrogen atoms and thus have a shorter atmospheric lifetime [1]. For these reasons, HFC mixtures have been considered as promising candidates for replacement of CFC compounds. Vapor–liquid equilibrium data are required as one of the most important types of information in evaluating the performance of refrigeration cycles and determining the optimum compositions of the working fluids. However, few experimental data have been reported previously in the literature for these systems.

In this work, we measured isothermal vapor–liquid equilibria for binary systems of HFC-32 + HFC-227ea and HFC-152a + HFC-227ea at 283.15 and 303.15 K and HFC-134a + HFC-227ea at 303.15 and 323.15 K in an apparatus in which both phases were continuously recirculated. The experimental data were correlated with the Peng–Robinson equation of state [2] using the Wong–Sandler mixing rule [3]. The interaction parameters, NRTL parameters, and average deviations of pressures and vapor phase compositions obtained by this equation of state were determined.

2. EXPERIMENTAL

2.1. Chemical/Purity

High-grade chemicals having purities greater than 99.8 mass%, as shown in Table I, were used for the measurements of VLE. The purities of the chemicals were certified by the manufacturers, and they were used without any further purification.

2.2. Vapor–Liquid Equilibrium Apparatus

Vapor–liquid equilibria were measured in an apparatus in which both vapor and liquid phases were continuously recirculated. The experimental apparatus used in this work is the same as that used in previous work [4–6] and is only briefly discussed here. A schematic diagram of the

Table I. Suppliers and Purities of the Pure Components

Component	Supplier	Purity (mass%)
HFC-32	DuPont	>99.8
HFC-134a	DuPont	>99.9
HFC-152a	DuPont	>99.9
HFC-227ea	Lancaster, UK	>99.9

apparatus is shown in Fig. 1. The equilibrium cell is a 316 stainless-steel vessel with an inner volume of about 85 cm^3. In its middle part, a pair of Pyrex glass windows of 20-mm thickness was installed so that the liquid level, mixing and circulating processes, and critical region phenomena could be observed during operation. A stirrer, rotated at variable speeds

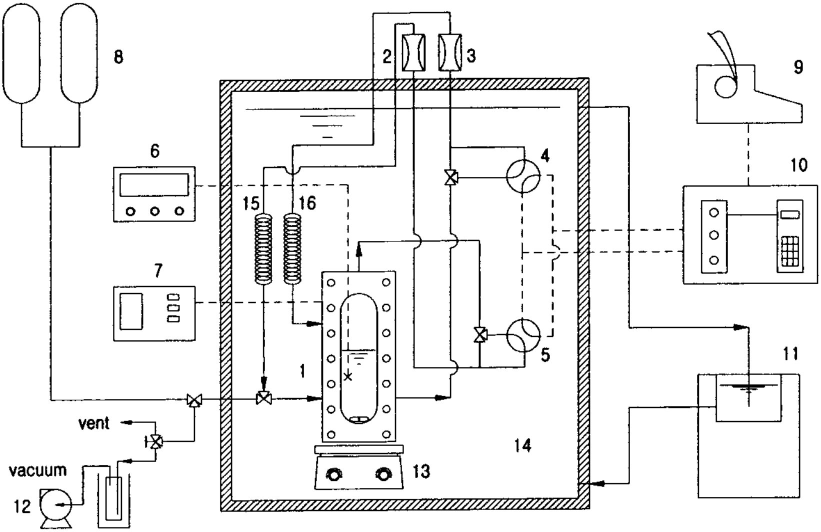

1. Equilibrium cell
2. Vapor circulation pump
3. Liquid circulation pump
4. Liquid sampling valve
5. Vapor sampling valve
6. Temperature indicator
7. Pressure indicator
8. Sample reservoir
9. Integrator
10. Gas chromatograph
11. Circulator
12. Vacuum pump
13. Magnetic stirrer
14. Constant-temperature water bath
15. Vapor-phase heat exchanger
16. Liquid-phase heat exchanger

Fig. 1. Schematic diagram of the experimental apparatus.

by an external magnet, was used to accelerate the attainment of the equilibrium state and to reduce concentration gradients in both phases.

The temperature of the equilibrium cell in the water bath was maintained by a circulator from Jeio Tech, Korea. The temperature in the cell was measured with a platinum resistance sensor and a digital temperature indicator Model F250MkII precision thermometer from Automatic Systems Laboratories Ltd., United Kingdom. They were calibrated by a NAMAS-accredited calibration laboratory. The uncertainty was estimated to be ±0.01 K. The total error in temperature measurements is estimated to be within 0.05 K, including the precision of the standard thermometer and the fluctuation of the temperature controller.

The pressure was measured with a pressure transducer, Model XPM60, and digital pressure calibrator, Model PC 106, from Beamax, Finland. Pressure calibrations are traceable to National Standards (Finland, Center for Metrology and Accreditation Cert. No. M-95P077, 14.11.1995, M-M 730, 16.11.1995, and M-95P078, 16.11.1995), and their uncertainties were estimated to be within ±0.005 MPa.

The vapor and liquid phases in the equilibrium cell were continuously recirculated by a dual-head circulation pump from the Milton Roy Company. When equilibrium was reached, the circulation pump was stopped and the pressure was measured. Then the vapor and liquid samples were withdrawn from the recycling loop and injected on-line into a Gow-Mac Model 550P gas chromatograph. The gas chromatograph was equipped with a thermal conductivity detector (TCD) and a Porapak Q column from Alltech Company.

2.3. Experimental Procedures

Experiments for a binary system were performed by the following procedure. The system was first evacuated to remove all inert gases. A targeted amount of HFC-227ea was introduced into the cell, and then the temperature of the entire system was maintained by controlling the temperature of the water bath. After the desired temperature was attained, the pressure of the pure component was measured. An appropriate amount of HFC-32 (for HFC-227ea + HFC-32) or HFC-134a (for HFC-227ea + HFC-134a) or HFC-152a (for HFC-227ea + HFC-152a) was supplied to the cell from a charging cylinder. The mixture in the cell was stirred continuously with the magnetic stirrer for over 1 h. Both vapor and liquid phases were recirculated by the dual-head circulation pump until an equilibrium state was established. It is believed that 1 h or more is sufficient to obtain thermal equilibrium between the cell fluid and the thermostated bath. After 1 h or more the pressure in the equilibrium cell was measured and then vapor and liquid samples were withdrawn from the recycling lines by the vapor and liquid sampling valves, respectively. The compositions of the samples were measured by immediately injecting them into the gas chromatograph, which was connected on-line to vapor and liquid sampling valves. The gas chromatograph was calibrated with pure components of known purity and with mixtures of known composition that were prepared gravimetrically. The experimental data at the equilibrium state were measured at least five times to ensure repeatability. Considering the margin of error and the reproducibility of GC, we generally estimated an overall uncertainty in the measurements of the composition of ± 0.002 in the mole fraction for both the liquid and the vapor phases.

3. RESULTS AND DISCUSSION

The VLE data were correlated with the Peng–Robinson (PR) equation of state [2], which is expressed as follows:

$$P = \frac{RT}{v-b} - \frac{a(T)}{v(v+b)+b(v-b)} \tag{1}$$

$$a(T) = \left(0.457235 \frac{R^2 T_c^2}{P_c}\right) \alpha(T) \tag{2}$$

$$\alpha(T) = [1 + \kappa(1 - \sqrt{T/T_c})]^2 \tag{3}$$

$$b = 0.077796 \frac{RT_c}{P_c} \tag{4}$$

$$\kappa = 0.37464 + 1.54226\omega - 0.26992\omega^2 \tag{5}$$

where the parameter a is a function of temperature, b is constant, κ is a constant characteristic of each substance, w is the acentric factor, P (in MPa)

Table II. Properties of the Pure Components[a]

Component	Chemical formula	MW	T_c (K)	P_c (MPa)	ω
HFC-32	CH_2F_2	52.02	351.26	5.782	0.2768
HFC-134a	CF_3CH_2F	102.03	374.21	4.059	0.3268
HFC-152a	CHF_2CH_3	66.05	386.41	4.517	0.2752
HFC-227ea	CF_3CHFCF_3	170.03	375.95	2.980	0.3632

[a] Data source: REFPROP (V. 6.01) [10].

Table III. Comparison of the Measured Pure Component Vapor Pressures with Calculated Values from REFPROP 6.01 [10]

Component	T (K)	P (MPa) Measured	P (MPa) REFPROP [10]	ΔP (MPa)[a]	$\lvert\Delta P\rvert/P$ (%)[b]
HFC-32	283.15	1.109	1.107	0.002	0.18
	303.15	1.924	1.928	−0.004	0.20
HFC-134a	303.15	0.770	0.770	0.000	0.00
	323.15	1.320	1.318	0.002	0.15
HFC-152a	283.15	0.373	0.372	0.001	0.26
	303.15	0.690	0.689	0.001	0.14
HFC-227ea	283.15	0.276	0.277	−0.001	0.36
	303.15	0.530	0.529	0.001	0.18
	323.15	0.922	0.921	0.002	0.21

[a] $\Delta P = P_{\mathrm{exp}} - P_{\mathrm{cal}}$.

[b] $\lvert\Delta P\rvert/P\ (\%) = \lvert P_{\mathrm{exp}} - P_{\mathrm{cal}}\rvert/P_{\mathrm{exp}} \times 100$.

Table IV. Vapor–Liquid Equilibrium Measurements for the HFC-32 (1) + HFC-227ea (2) System

P (MPa)	x_1	y_1	PR $\Delta P/P$ (%)[a]	PR Δy[b]	REFPROP [10] $\Delta P/P$ (%)[a]	REFPROP [10] Δy[b]
			$T = 283.15$ K			
0.2775	0.0000	0.0000	1.4100	0.0000	−1.730	0.0000
0.4418	0.1714	0.4424	−0.1154	−0.0101	−5.750	−0.0129
0.5382	0.2790	0.5850	0.2657	−0.0099	−4.550	0.0319
0.5844	0.3320	0.6363	0.0530	−0.0142	−3.570	0.0289
0.6720	0.4320	0.7186	−0.3378	−0.0178	−1.200	0.0220
0.7750	0.5476	0.7905	−0.1703	−0.0210	1.830	0.0054
0.8360	0.6159	0.8280	0.3050	−0.0186	3.410	−0.0035
0.9194	0.7312	0.8832	−0.3621	−0.0126	3.400	−0.0063
0.9962	0.8240	0.9240	0.7046	−0.0063	3.880	−0.0143
1.1092	1.0000	1.0000	−0.4309	0.0000	−0.045	−0.0038
			$T = 303.15$ K			
0.5303	0.0000	0.0000	1.9376	0.0000	−0.848	0.0000
0.7354	0.1386	0.3428	−0.1128	−0.0038	−4.560	−0.0037
0.8724	0.2308	0.4849	0.2189	−0.0040	−3.800	0.0091
1.0104	0.3278	0.5901	−0.0475	−0.0101	−2.640	0.0139
1.1310	0.4113	0.6647	−0.1008	−0.0123	−1.090	0.0188
1.3284	0.5480	0.7594	−0.1038	−0.0171	1.360	0.0186
1.5104	0.6741	0.8320	0.2085	−0.0162	3.000	0.0149
1.7218	0.8339	0.9152	−0.0558	−0.0085	2.650	0.0069
1.9240	1.0000	1.0000	−1.1382	0.0000	−0.369	−0.0040

[a] $\Delta P/P\ (\%) = (P_{\mathrm{exp}} - P_{\mathrm{cal}})/P_{\mathrm{exp}} \times 100$.

[b] $\Delta y = y_{\mathrm{exp}} - y_{\mathrm{cal}}$.

is the pressure, P_c (in MPa) is the critical pressure, T (in K) is the absolute temperature, T_c (in K) is the critical temperature, T_r is the reduced temperature, and v is the molar volume.

The Wong–Sandler mixing rule [3] was used in this work to obtain equation-of-state parameters for a mixture from those of the pure components. Wong and Sandler equated the excess Helmholtz free energy at infinite pressure from an equation of state to the excess Helmholtz free energy from any activity coefficient model, in such a way that a mixing rule is obtained which simultaneously satisfies the quadratic composition dependence of the second virial coefficient but also behaves like an activity

Table V. Vapor–Liquid Equilibrium Measurements for the HFC-134a (1) + HFC-227ea (2) System

			PR		REFPROP [10]	
P (MPa)	x_1	y_1	$\Delta P/P$ (%)^a	Δy^b	$\Delta P/P$ (%)^a	Δy^b
			$T = 303.15$ K			
0.5303	0.0000	0.0000	1.9366	0.0000	0.244	0.0000
0.5470	0.0555	0.0825	0.0256	−0.8128	−1.670	−0.0084
0.6096	0.2792	0.3557	−0.1181	0.0007	−5.190	−0.0118
0.6402	0.3890	0.4647	0.1655	−0.0104	−5.220	−0.0124
0.6686	0.4992	0.5702	0.0867	−0.0157	−4.800	−0.0062
0.6972	0.6275	0.6871	−0.3442	−0.0134	−4.130	0.0050
0.7208	0.7232	0.7688	−0.0042	−0.0096	−2.820	0.0122
0.7390	0.8026	0.8429	0.3004	0.0021	−1.690	0.0249
0.7624	0.9548	0.9607	−0.0931	−0.0015	−0.574	0.0079
0.7700	1.0000	1.0000	0.0234	0.0000	−0.039	0.0000
			$T = 323.15$ K			
0.9210	0.0000	0.0000	0.0139	0.0000	−0.141	0.0000
1.0260	0.2704	0.3332	0.1413	−0.0106	−6.510	−0.0090
1.0806	0.3926	0.4531	−0.1897	−0.0265	−6.610	−0.0120
1.1066	0.4481	0.5059	−0.1346	−0.0295	−6.240	−0.0115
1.1414	0.5202	0.5727	0.1524	−0.0304	−5.430	−0.0100
1.2028	0.6771	0.7133	0.0407	−0.0245	−4.190	−0.0011
1.2492	0.7981	0.8232	0.1969	−0.0136	−2.690	0.0103
1.2748	0.8750	0.8920	0.0196	−0.0075	−1.830	0.0148
1.2934	0.9455	0.9487	−0.5574	−0.0080	−1.270	0.0059
1.3201	1.0000	1.0000	−0.1128	0.0000	0.197	−0.0120

[a] $\Delta P/P\ (\%) = (P_{exp} - P_{cal})/P_{exp} \times 100$.

[b] $\Delta y = y_{exp} - y_{cal}$.

coefficient model at high density [7]. This mixing rule for a cubic equation of state can be written

$$b_m = \frac{\sum_i \sum_j x_i x_j (b - a/RT)_{ij}}{(1 - A^{\mathrm{E}}_{\infty}/CRT - \sum_i x_i a_i/RTb_i)} \tag{6}$$

with

$$(b - a/RT)_{ij} = \tfrac{1}{2}[(b - a/RT)_i + (b - a/RT)_j](1 - k_{ij}) \tag{7}$$

Table VI. Vapor–Liquid Equilibrium Measurements for the HFC-152a (1) + HFC-227ea (2) System

			PR		REFPROP [10]	
P (MPa)	x_1	y_1	$\Delta P/P$ (%)[a]	Δy[b]	$\Delta P/P$ (%)[a]	Δy[b]
			$T = 283.15$ K			
0.2775	0.0000	0.0000	1.4126	0.0000	0.244	0.0000
0.2899	0.1437	0.1686	0.9486	−0.0144	−1.670	−0.0084
0.3007	0.2772	0.3310	−0.3658	−0.0135	−5.190	−0.0118
0.3184	0.4419	0.5103	−0.7160	−0.0123	−5.220	−0.0124
0.3413	0.6341	0.7091	−0.0381	0.0086	−4.800	−0.0062
0.3528	0.7408	0.7945	0.3004	0.0049	−4.130	0.0050
0.3623	0.8432	0.8606	0.4526	−0.0115	−2.820	0.0122
0.3670	0.9065	0.9176	0.3624	−0.0055	−1.690	0.0249
0.3714	0.9662	0.9698	0.3742	−0.0020	−0.574	0.0079
0.3733	1.0000	1.0000	0.2705	0.0000	−0.039	0.0000
			$T = 303.15$ K			
0.5303	0.0000	0.0000	1.9366	0.0000	−0.141	0.0000
0.5472	0.1599	0.1862	0.4203	−0.0090	−6.510	−0.0090
0.5739	0.3262	0.3869	0.3310	−0.0015	−6.610	−0.0120
0.6028	0.4693	0.5392	0.1476	0.0006	−6.240	−0.0115
0.6354	0.6386	0.6974	0.0031	0.0006	−5.430	−0.0100
0.6554	0.7461	0.7880	0.2303	−0.0012	−4.190	−0.0011
0.6730	0.8619	0.8780	0.1456	−0.0071	−2.690	0.0103
0.6824	0.9345	0.9405	0.0117	−0.0046	−1.830	0.0148
0.6874	0.9875	0.9900	0.2734	0.0006	−1.270	0.0059
0.6901	1.0000	1.0000	0.1086	0.0000	0.197	−0.0120

[a] $\Delta P/P\ (\%) = (P_{\mathrm{exp}} - P_{\mathrm{cal}})/P_{\mathrm{exp}} \times 100$.

[b] $\Delta y = y_{\mathrm{exp}} - y_{\mathrm{cal}}$.

and

$$\frac{a_m}{b_m}=\sum_i x_i\frac{a_i}{b_i}+\frac{A_\infty^{\mathrm{E}}}{C} \tag{8}$$

where C is a numerical constant equal to $\ln(\sqrt{2}-1)/\sqrt{2}$ for the Peng–Robinson equation [2] used in this work. Also, A_∞^{E} is an excess Helmholtz free energy at infinite pressure that can be equated to a low-pressure excess Gibbs free energy [8]; in this study we use the NRTL model [9] given by

$$\frac{A_\infty^{\mathrm{E}}}{RT}=\sum_i x_i\frac{\sum_j x_j G_{ji}\tau_{ji}}{\sum_k x_k G_{ki}} \tag{9}$$

with

$$G_{ji}=\exp(-\alpha_{ij}\tau_{ji}) \qquad \text{and} \qquad \tau_{ij}=A_{ij}/(RT) \tag{10}$$

where G_{ij} is the local composition factor for the NRTL model, τ_{ij} is the NRTL model binary interaction parameter, $A_{ij}=(g_{ij}-g_{jj})$, where g_{ij} is an interaction energy parameter of the i–j component, α_{ij} is a nonrandomness

Table VII. Interaction Parameters, NRTL Parameters, and Average Deviations of P and y

				PR		REFPROP [10]	
T (K)	f_{12}	A_{12}[a]	A_{21}[a]	AADP (%)[b]	δy[c]	AADP (%)[b]	δy[c]
			HFC-32 + HFC-227ea				
283.15	0.334	6.112	−3.414	0.41	0.0110	3.25	0.0139
303.15	0.254	4.387	−2.652	0.43	0.0082	2.51	0.0099
			HFC-134a + HFC-227ea				
303.15	0.295	8.648	−4.872	0.33	0.0061	2.65	0.0088
323.15	0.354	−2.289	−0.274	0.29	0.0150	3.50	0.0088
			HFC-152a + HFC-227ea				
283.15	0.159	0.710	−1.336	0.52	0.0080	1.72	0.0111
303.15	0.148	0.592	−1.319	0.36	0.0025	1.87	0.0087

[a] The unit of A_{12} and A_{21} is $\mathrm{kJ\cdot mol^{-1}}$.

[b] $\mathrm{AADP}\ (\%)=(1/N)\sum|(P_{\mathrm{exp}}-P_{\mathrm{cal}})/P_{\mathrm{exp}}|\times 100$.

[c] $\delta y=(1/N)\sum|y_{\mathrm{exp}}-y_{\mathrm{cal}}|$.

parameter, and R is the universal gas constant ($8.314\ \mathrm{J \cdot K^{-1}\, mol^{-1}}$). The critical properties (T_c, P_c) and acentric factors (ω) of HFC-32, HFC-134a, HFC-152a, and HFC-227ea used to calculate the parameters for the Peng–Robinson equation of state are given in Table II. We have set the nonrandomness parameter, α_{ij}, equal to 0.3 for all the binary mixtures studied here. The parameters of these equations were obtained by minimizing the following objective function:

$$\text{objective function} = \frac{1}{N} \sum_{j}^{N} \left[\left(\frac{P_{j,\,\mathrm{exp}} - P_{j,\,\mathrm{cal}}}{P_{j,\,\mathrm{exp}}} \right) \times 100 \right]^2 \qquad (11)$$

where N is the number of experimental points, P_{exp} is the experimental pressure, and P_{cal} is the calculated pressure.

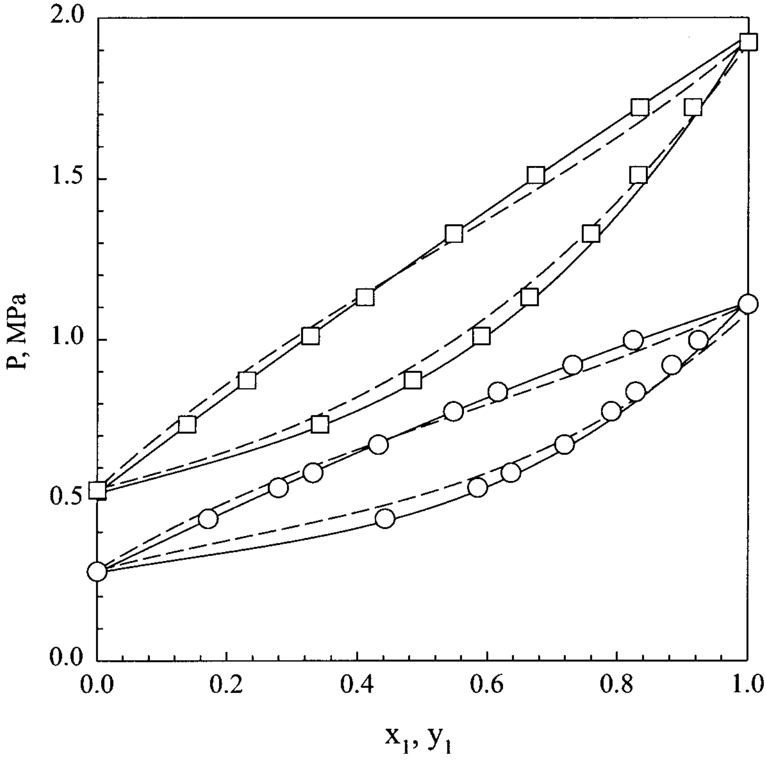

Fig. 2. Comparisons of experimental (expt) data with VLE correlation of the HFC-32 + HFC-227ea binary system. (○) Expt at 283.15 K; (□) expt at 303.15; (——) correlated by PR; (- - - -) correlated by REFPROP [10].

Table III provides comparisons of measured saturated vapor pressures of pure HFC-32, HFC-134a, HFC-152a, and HFC-227ea with those calculated from REFPROP 6.01 [10], which is considered to be reliable for the pure compounds considered here and consistent with other literature data. The deviations (ΔP) between measured and calculated values were within ± 0.005 MPa for all components and the average absolute deviation ($\Delta P/P$) was 0.19% for HFC-32, 0.075% for HFC-134a, 0.20% for HFC-152a, and 0.25% for HFC-227ea.

The experimental isothermal VLE data for the binary systems of HFC-32 + HFC-227ea at 283.15 and 303.15 K, HFC-134a + HFC-227ea at 303.15 and 323.15 K, and HFC-152a + HFC-227ea at 283.15 and 303.15 K are shown in Tables IV, V, and VI, respectively. Each table lists the measured mole fractions of the liquid and vapor phases, pressures, and temperatures at equilibrium and the deviation of the correlated value using PR

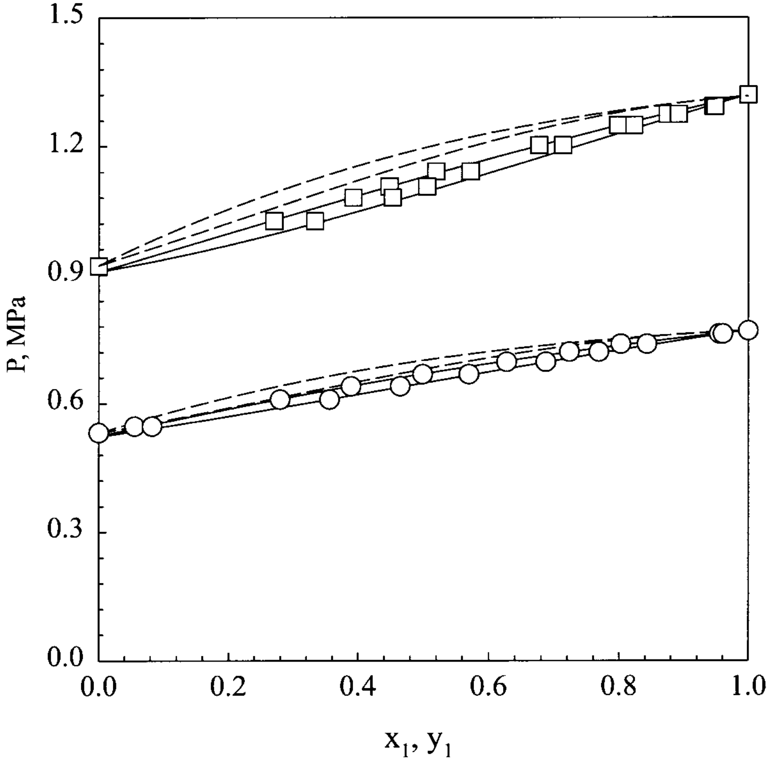

Fig. 3. Comparisons of experimental (expt) data with VLE correlation of the HFC-134a + HFC-227ea binary system. (○) Expt at 303.15 K; (□) expt at 323.15; (——) correlated by PR; (- - - -) correlated by REFPROP [10].

equation-of-state and REFPROP results [10] at each point. Figures 2–4 show comparisons of measured and calculated values using Peng–Robinson equation-of-state and REFPROP results [10] for these three binary systems. The interaction parameters, the parameters of NRTL activity coefficient model in the PR equation of state, and the average absolute deviations of pressure (AAD-P) and vapor phase composition (δy) between measured and calculated values and between measured and REFPROP values [10] are provided in Table VII. Figure 5–7 show the deviations of the correlated values using PR equation-of-state and REFPROP results [10] at each point. The overall deviations of pressure using the PR equation of state were 0.42% for HFC-32 + HFC-227ea, 0.31% for HFC-134a + HFC-227ea, and 0.44% for HFC-152a + HFC-227ea system, and those using REFPROP [10] were 2.88% for HFC-32 + HFC-227ea, 3.08% for HFC-134a + HFC-227ea, and 1.80% for HFC-152a + HFC-227ea system.

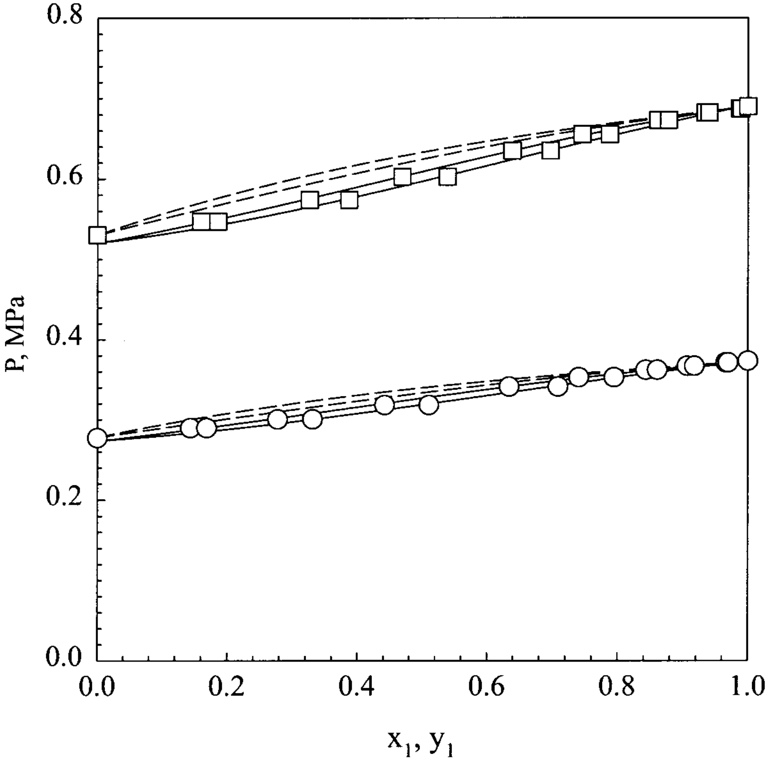

Fig. 4. Comparisons of experimental (expt) data with VLE correlation of the HFC-152a + HFC-227ea binary system. (○) Expt at 283.15 K; (□) expt at 303.15; (——) correlated by PR; (- - - -) correlated by REFPROP [10].

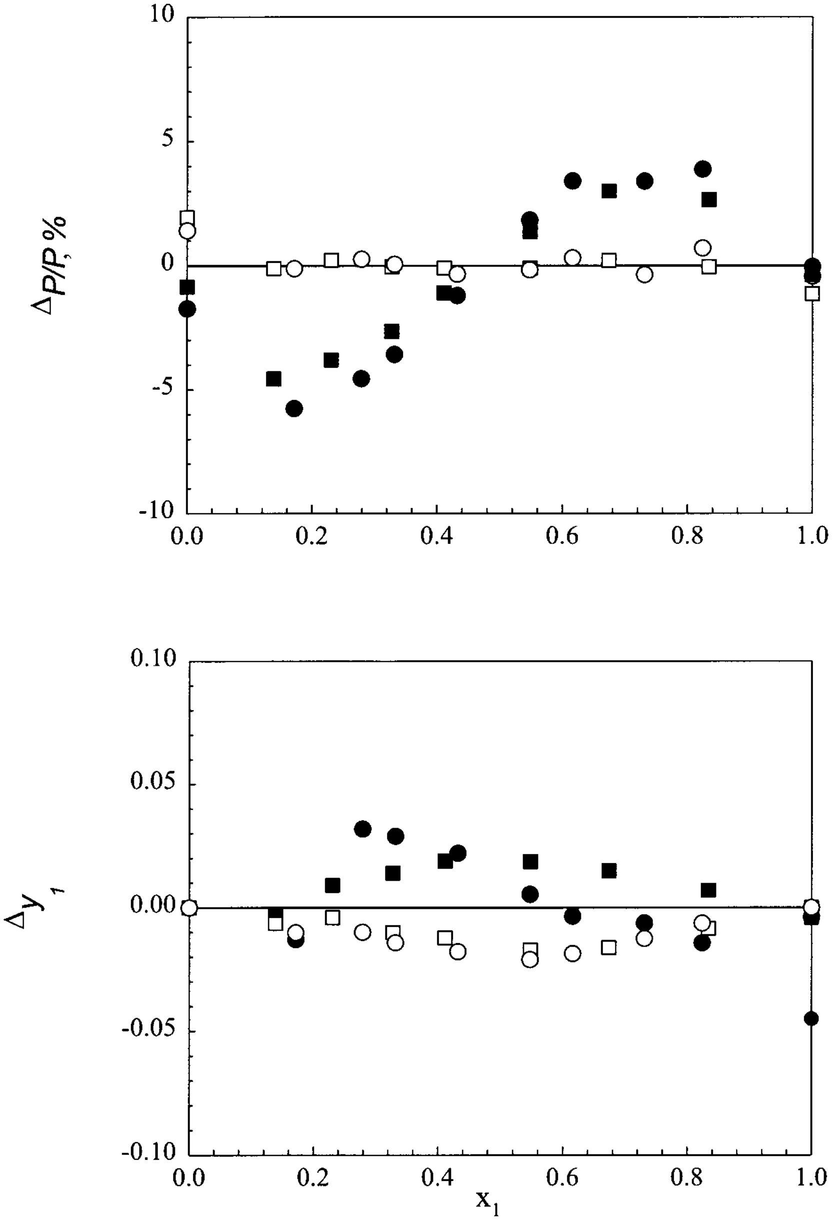

Fig. 5. Deviations of pressure and vapor composition for the system HFC-32 + HFC-227ea: (○) PR at 283.15 K; (■) PR at 303.15 K; (●) REFPROP [10] at 283.15 K; (■) REFPROP [10] at 303.15 K.

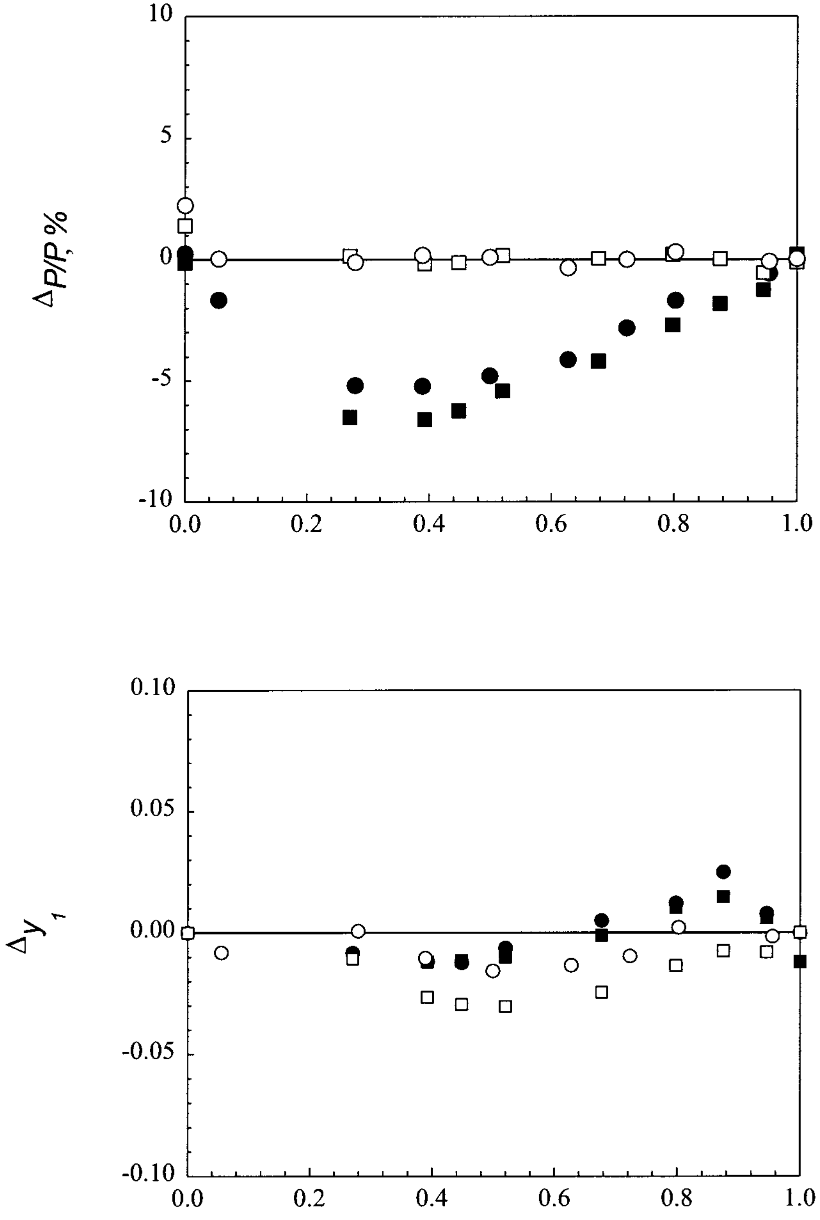

Fig. 6. Deviations of pressure and vapor composition for the system HFC-134a + HFC-227ea: (○) PR at 303.15 K; (■) PR at 323.15 K; (●) REFPROP [10] at 303.15 K; (■) REFPROP [10] at 323.15 K.

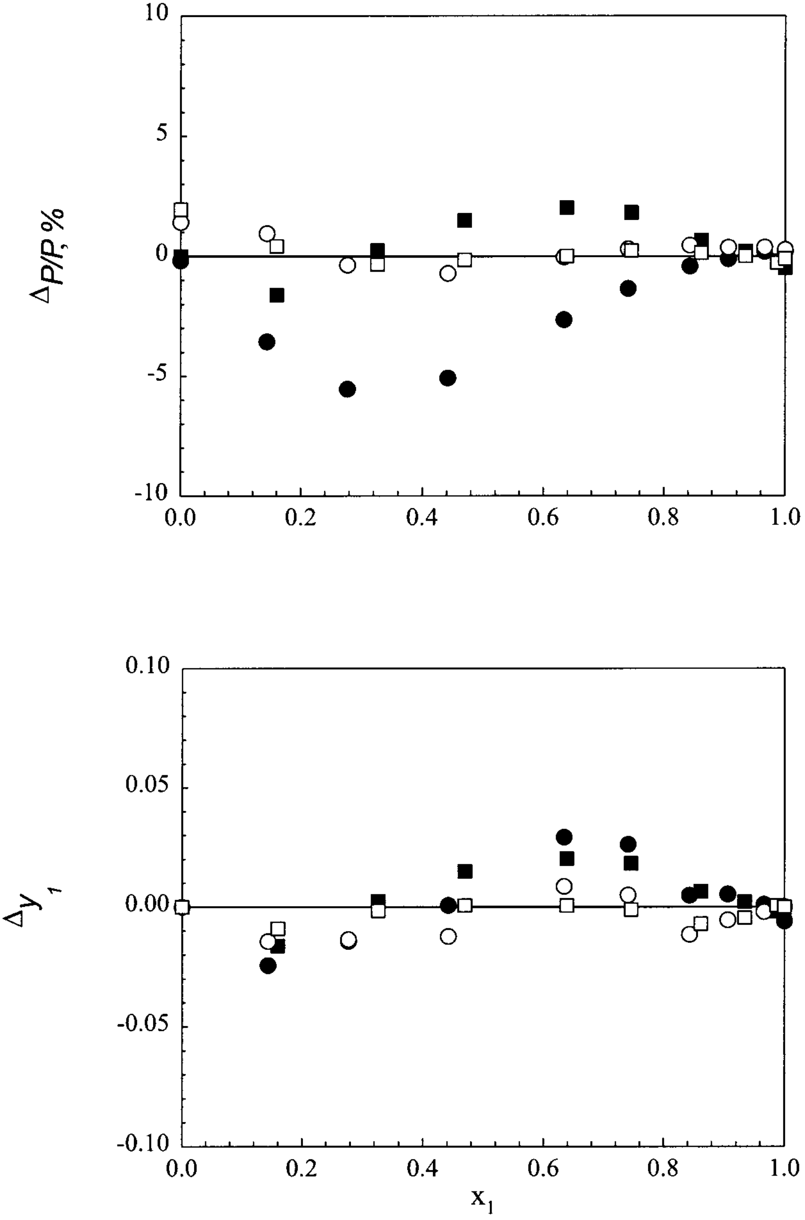

Fig. 7. Deviations of pressure and vapor composition for the system HFC-152a + HFC-227ea: (○) PR at 283.15 K; (■) PR at 303.15 K; (●) REFPROP [10] at 283.15 K; (■) REFPROP [10] at 303.15 K.

Our experimental data have shown relatively good agreement with the calculated values using the PR equation of state with the Wong–Sandler mixing. Azeotropic behavior has not been found in any of these mixtures.

4. CONCLUSIONS

We measured vapor–liquid equilibria for binary systems of HFC-32 + HFC-227ea, HFC-134a + HFC-227ea, and HFC-152a + HFC-227ea. The Peng–Robinson equation of state with the Wong–Sandler mixing rule has given satisfactory results in comparison with the experimental data. An azeotropic composition was not found for any of the mixtures studied here.

NOMENCLATURE

$a(T)$	Temperature-dependent equation-of-state constant
b	Equation-of-state constant
k	Peng–Robinson equation-of-state parameter
P, P_c	Pressure, critical pressure (MPa)
R	Gas constant, 8.3144 $J \cdot mol^{-1} K^{-1}$
T, T_c, T_r	Absolute temperature, critical temperature, reduced temperature (K)
x	Liquid mole fraction
y	Vapor mole fraction
v	Liquid molar volume

Greek Letters

$\alpha(T)$	Temperature-dependent equation-of-state parameter
ω	Acentric factor

Subscripts

c	Critical property
cal	Calculated
exp	Experimental
i, j	ith, jth component of the mixture

REFERENCES

1. M. Lisal and V. Vacek, *Fluid Phase Equil.* **118**:61 (1996).
2. D. Y. Peng and D. B. Robinson, *Int. Eng. Chem. Fundam.* **15**:59 (1976).
3. D. S. H. Wong and S. I. Sandler, *AIChE J.* **38**:671 (1992).

4. B. G. Lee, J. Y. Park, J. S. Lim, S. Y. Cho, and K. Y. Park, *J. Chem. Eng. Data* **44**:190 (1999).
5. J. S. Lim, J. Y. Park, B. G. Lee, W. Y. Lee, and J. D. Kim, *J. Chem. Eng. Data* **44**:1226 (1999).
6. J. S. Lim, J. Y. Park, and B. G. Lee, *Int. J. Thermophys.* **21**:1339 (2000).
7. H. Huang, S. I. Sandler, and H. Orbey, *Fluid Phase Equil.* **96**:143 (1994).
8. D. S. H. Wong, H. Orbey, and S. I. Sandler, *Ind. Eng. Chem. Res.* **31**:2033 (1992).
9. H. Renon and J. M. Prausnitz, *AIChE J.* **14**:5 (1968).
10. M. Huber, J. Gallagher, M. O. McLinden, and G. Morrison, *Thermodynamic Properties of Refrigerants and Refrigerant Mixtures Database*, REFPROP V. 6.01 (National Institute of Standards and Technology, Boulder, CO, 1996).